Comparative application of an irradiated and non-irradiated calcite-type material to improve the removal of Pb in batch and continuous processes

Julian Cruz-Olivares[a,b,*], Carlos E. Barrera-Díaz[a], Gonzalo Martínez-Barrera[a], César Pérez-Alonso[a], Gabriela Roa-Morales[a]

[a] Facultad de Química, Universidad Autónoma del Estado de México, Paseo Colón esq, Paseo Tollocan S/N, 50120, Toluca, Estado de México, Mexico
[b] MCCM Ciencia e Innovación Tecnológica S.A. de C.V., Av. Benito Juárez Sur 1002, Col. Universidad, C.P. 50130, Toluca, Estado de México, Mexico

ARTICLE INFO

ABSTRACT

The study compared the lead adsorption capacity of an irradiated and non-irradiated calcite-type material carried out in simulated wastewater. The adsorption capacity in the batch process was evaluated at different temperatures and initial concentrations. The equilibrium adsorption was fitted with the Langmuir and Dubinin – Radushkevich models. Kinetic results were described by the pseudo-second order and intraparticle-diffusion models. The thermodynamic parameters were evaluated as well. The highest adsorption capacity in the batch process (4.808 mg/g) was found at 40 °C, with 100 mg/L as initial concentration. The study was also conducted in a continuous mode using only the irradiated material, owing to its high adsorption capacity compared with the non-irradiated one. The effects of flow rate (5, 7.5 and 10 mL/min), initial concentration (60, 80 and 100 mg/L) and bed height (5, 7.5 and 10 cm) were evaluated. The highest adsorption capacity in the continuous process (4.602 mg/g) was achieved at 40 °C, with a 100 mg/L lead initial concentration solution, within a flow rate of 5 mL/min and a bed depth of 10 cm. The breakthrough time for a lead concentration at the exit of the column equal to 1 mg/L was 232.65 min. In this case, the effective mass transfer zone (MTZ) in the packed bed was 5.7 cm for a treated volume of 1163.25 mL and a lead removal of 86.98%. The column experimental results, in terms of the breakthrough curve, were better fitted with the Thomas and Yoon - Nelson models than with Dose – Reponse model.

1. Introduction

Although the pollution of water by heavy metals has been matter of study for many important groups of environmental researchers, it still remains as a large problem to be solved. Among heavy metals, people identify lead as the worst pollutant. Apart from that, it has been reported that lead, even in small quantities, can damage some vital organs of living organisms and cause serious illnesses to human beings, especially children. Today, many pediatric diseases are attributed to the exposure of children to a large number of chemical compounds dispersed in soil, air and water [1,2].

It is well known that exposure to lead causes severe damage to health, mainly in children but also in adults who are exposed to moderate concentrations; for example, damage in cardiovascular end points. Such exposure infers a causal relationship between lead exposure and hypertension [2].

In many underdeveloped countries with poor environmental regulations, where industries continue to discharge wastewater into rivers, there appears the opportunity to propose economic but effective processes to solve this problem, mainly in microindustries such as pottery, tannery and electroplating, among others [3,4].

The effective removal of heavy metal ions from wastewater is a goal of environmental departments in many industries and is also the subject of studies for many researchers. Adsorption is one of the technologies that has proved highly effective in removing metal ions from wastewater. This technology, unlike others such as electrocoagulation, chemical precipitation, nanofiltration, is safe and inexpensive, as long as the adsorbent is a waste material or does not require subsequent conditioning [5,6]. In several metal adsorption works, adsorbents of agro-industrial waste, called bioadsorbents, are commonly studied. Due to their nature and scarce physicochemical treatment, these bioadsorbents are considered low cost [7–10]. Inorganic, natural or synthetic materials, with or without physical-chemical treatments, are also used as adsorbents. This kind of materials are more promising owing to their

---

high mechanical resistance, their insolubility in water and the possibility of being reused [11–14].

Gamma irradiation has a lot of applications in novel industrial processes. This technology is used commercially for food preservation, industrial applications handling organic and inorganic materials, as well as for quarantine purposes, particularly soil materials. When gamma irradiation is applied to solid inorganic materials, several effects are produced on their chemical structure as well as on their physical and chemical properties. For example, effects on the lattice and atomic dislocations are produced. Moreover, in specific applications it has been an adequate tool with great success, for example, hydrolysis of water into oxidizing and reducing species which may change the oxidation–reduction potential of soil water [15]. Even though there is a lack of investigations that address the application of gamma radiation as a modifier of adsorbent materials, in a previous work it was found that the adsorption capacity of a mineral increases slightly as the gamma radiation dose increases [11]. It is expected that structural changes on the irradiated solids would be responsible for the increase in the adsorption capacity. There are no adverse effects reported for humans who interact with gamma irradiated materials, owing to the nature of gamma rays, this is to say, the interactions of gamma rays with a solid material diminish their intensity in terms of the penetrated distance, their maximum effectivity is around 10 cm, but for longer distances, energy intensity gradually diminishes and eventually their effect disappears.

In environmental engineering, there are two ways to operate the process of adsorption of metal ions: batch and continuous operations. In batch processes, the process variables are perfectly controlled, so it is easy to reach equilibrium and obtain the kinetic, thermodynamic and transport parameters [16–18]. This information is then used to design the continuous processes, which are preferred to treat large volumes of effluent [19,20].

The equilibrium studies for adsorption processes can be modeledby means of equations such as Langmuir, Freundlich, Dubinin – Radushkevich, among others [21,22]. These models, also called adsorption isotherms, describe the interaction between the substance that must be absorbed and the adsorbent material. This interaction takes place on the surface of the adsorbent and, therefore, provides information on the adsorption capacity of the adsorbent material [23,24]. In most cases, the kinetics of adsorption processes can be described by simple models such as Lagergren's and Ho's, also known as kinetic models of pseudo-first order and pseudo-second order, respectively. Other models such as Elovich, intraparticle- diffusion and Bangham's kinetics models are also used [16,25,26]. In like manner, for the thermodynamic parameters, once the distribution coefficient is experimentally obtained for each temperature, by means of the Van't Hoff and Clausius – Clapeyron equations, standard enthalpy, standard entropy, standard free energy and isosteric heat of adsorption can be calculated [27–29]. All of these studies are carried out in batch process.

The continuous system has many advantages over the batch process and can therefore be used at an industrial scale. In this process, packed columns are used; either fixed bed or fluidized bed [30]. In order to model a continuous system, simplified equations are resorted to such as the Thomas model, the Yoon – Nelson model, the Adams – Bohart model, among others, which in many cases reproduce the column adsorption processes in a satisfactory manner [31–33].

In this work, non-irradiated and irradiated materials utilized as adsorbents to remove lead ions from simulated wastewater were compared. Furthermore, the equilibrium, kinetic and thermodynamic parameters were estimated in order to analyze the effect of experimental variables, such as equilibrium time, temperature, and initial concentration, in both kind of materials.

Adsorption was carried out in batch and continuous processes. In the batch process, the effects of gamma irradiation (0, 200kGy), temperature (20, 30 and 40 °C) and initial concentration (10, 20, 40, 60, 80 and 100 mg/L) were analyzed in order to find the maximum adsorption

capacity and removal percentage. The kinetic of the process was modelled using pseudo-second order and intraparticle-diffusion models, while the equilibrium adsorption was modelled using the Langmuir and Dubinin – Radushkevich equations. The thermodynamic parameters of the adsorption process were also calculated. In the continuous process, the effects of initial concentration (60, 80 and 100 mg/l), flow rate (5, 7.5 and 10 ml/min) and bed depth (5, 7.5 and 10 cm) on the adsorption capacity and lead removal percentage in a fixed-bed column were studied. In this case, the process was successfully modelled by the Thomas, Yoon – Nelson and Dose – Reponse models.

2. Materials and methods

2.1. Preparation of non-irradiated and irradiated adsorbents

The natural material utilized in this work was extracted from mines located in Oaxaca, Mexico, and was purchased from an enterprise called Lumogral S.A. de C.V (located in Iztapalapa, Mexico City). This material was selected as adsorbent, because according to the seller it had been already utilized as a sieve in wastewater treatment plants in Mexico City. This shows low solubility in water and excellent mechanical properties, such characteristics were considered in order to explore its adsorption capacity to remove lead ions.

The material was trilled and sieved down to a particle size range of 0.149 - 0.177 mm. The non-irradiated adsorbent was obtained by washing the selected material at 40 °C in deionized water and drying it at 60 °C for 12 h in an electric oven. The irradiated adsorbent was obtained when the material was exposed to gamma radiation. The radiation process (200 kGy, 3.5 kGy/h) was performed at room temperature by using a Transelektro irradiator LGI-01 manufactured by IZOTOP Institute of Isotopes Co. Ltd., Budapest, Hungary.

The physicochemical characterization of this material (morphological surface, semi-quantitative elemental analysis and X-Ray diffraction) has been previously reported [11]. X-Ray analysis indicates that its chemical elements belong to calcite, calcium magnesium silicate and quartz.

2.2. Preparation of lead solutions

Aqueous solutions at a concentration of 100 mg/L of lead were prepared by dissolving dried salt (159.8 mg) of analytical grade lead nitrate [Pb(NO$_3$)$_2$] in deionized water (1 L). From this, other solutions at different concentrations (10, 20, 40, 60, 80 and 100 mg/L) were obtained by dilution. These aqueous lead solutions will be in contact with the adsorbent in the batch as well as in the continuous process. Once the material is saturated with lead ions, it is washed with an acidic aqueous solution to be reused, the leachates are confined in suitable containers for final disposal in authorized sanitary landfills.

2.3. Batch lead adsorption experiments

After the preparation of lead solutions, in 100 mL of such solution, 1.0 g of adsorbent was added. These heterogeneous mixtures were heated at constant temperature (20, 30 and 40 °C) and stirred with a shaker at 100 rpm (Lab-Line Incubator-Shaker, USA) until equilibrium was reached. Finally, separations of solid adsorbents were obtained by means of a filtration process. The concentrations of metals into the liquid solutions were analyzed by using Atomic Absorption Spectrophotometer (Perkin-Elmer model AA300), according to the standard method for lead detection [34].

The adsorption capacity, q (mg/g) was calculated with:

$$q = \frac{(C_0 - C_e)V}{w}$$

Where C_0 and C_e (mg/L) are the concentrations of lead at initial and equilibrium times, respectively; V (L) is the volume of the solution and

w (g) is the mass of the adsorbent.

The percentage of lead removal (%R) was obtained according to the following equation:

$$\%R = \left[\frac{(C_0 - C_e)}{C_0} \right] \times 100$$

2.4. Kinetic of adsorption process

2.4.1. Pseudo-second order model

Generally speaking, the dynamic of the adsorption process in the batch mode is represented by means of simplified models such as Lagergren or pseudo-first order and Ho pseudo-second order [35].

The pseudo-second order model is described by the following equation:

$$\frac{dq}{dt} = k_2 (q_e - q)^2$$

Where k_2 (g/mg·min) is the kinetic constant of second-order adsorption, q_e is the adsorption capacity at equilibrium (mg/g)

The integrated equation for such model is represented by the equation of straight line:

$$\frac{t}{q} = \left(\frac{1}{q_e} \right) t + \frac{1}{k_2 \bullet q_e^2}$$

2.4.2. Intraparticle diffusion model

When the adsorption seems to be controlled by the speed of diffusion within the particle, the adsorption speed of the batch process can be analyzed by the intraparticle diffusion model proposed by Uranus and Tachikawa [36]:

$$-ln \left[1 - \left(\frac{q}{q_e} \right)^2 \right] = \left(\frac{4\pi^2 D}{d_p^2} \right) t$$

Where D is the diffusion coefficient in the solid (m²/s)

2.5. Equilibrium of adsorption process

2.5.1. Langmuir isotherm

Langmuir isotherm quantitatively describes the formation of an adsorbate monolayer on the outer surface of the adsorbent.

$$q_e = \frac{q_0 K_L C_e}{1 + K_L C_e}$$

where q_e is the adsorption capacity, *i.e.*, the amount of lead adsorbed by the mineral at equilibrium (mg/g), C_e is the concentration of lead at equilibrium (mg/L), q_0 is the maximum adsorption capacity covered by a monolayer (mg/g), K_L is the constant of the Langmuir isotherm (L/mg) and R_L is a parameter of the Langmuir isotherm that indicates the nature of the adsorption.

$$R_L = \frac{1}{1 + K_L C_0}$$

R_L	Type of Adsorption
$R_L > 1$	Not favorable
$R_L = 1$	Linear
$0 < R_L < 1$	Favorable
$R_L = 0$	Irreversible

2.5.2. Dubinin – Radushkevich isotherm

This isotherm makes it possible to infer the mechanism of the adsorption process with a Gaussian-type energy distribution on a heterogeneous surface.

$$q_e = q_s e^{-K_{ads} \varepsilon^2}$$

where q_e is the theoretical saturation adsorption capacity (mg/g), q_s is the adsorption capacity, *i.e.*, the amount of lead adsorbed by the material at equilibrium (mg/g), K_{ads} is the adsorption constant of the Dubinin – Radushkevich isotherm (mol²/kJ²) and ε is a constant of the Dubinin – Radushkevich isotherm.

$$\varepsilon = RT \, Ln \left(1 + \frac{1}{C_e} \right)$$

Where R is the universal gas constant (8.314 J/mol), T is the absolute temperature (K) and C_e is the concentration of lead at equilibrium (mg/L).

With this isotherm an adsorption constant is obtained, which is used to distinguish physical adsorption from chemical adsorption of the metal ions with their free energy (E) per molecule of adsorbate (to remove a molecule from its position in the space of adsorption to the fluid bulk).

$$E = \frac{1}{\sqrt{2K_{ads}}}$$

$$q_e = q_s e^{-K_{ads} \varepsilon^2}$$

2.6. Determination of thermodynamic parameters

The thermodynamic properties are obtained by varying the equilibrium constant of the adsorption process (K_{ads}), a parameter that is also known as distribution coefficient. K_{ads} depends on temperature and is obtained through the following expression:

$$K_{ads} = \frac{q_e}{C_e}$$

Where q_e and C_e are the adsorption capacity and concentration in the balance, respectively. K_{ads} is related to Gibbs free energy by the following thermodynamic equation:

$$\Delta G^0 = -RTlnK_{ads}$$

The enthalpy and entropy of the adsorption process are calculated using the Van't Hoff equation.

$$lnK_{ads} = \frac{\Delta S^0}{R} - \frac{\Delta H^0}{RT}$$

Where R (8.314 J/molK) is the universal constant of the gases, while T (K) is the absolute temperature at which the adsorption process is carried out.

Isosteric heat is the heat of adsorption at a constant surface area. This depends on the fraction of adsorbent covered by adsorbate at each temperature and is related to the concentration at equilibrium by the following equation [37]:

$$\left(\frac{dlnC_e}{dT} \right) = -\frac{\Delta H_{st}}{RT^2}$$

The isothermal heat of adsorption ΔH_{st} is calculated from the slope of the line obtained by plotting lnC_e against $(1 / T)$ for the different concentrations adsorbed.

2.7. Column lead adsorption experiments

The experiments of continuous process were carried out using a glass column (1.78 cm ID, 30 cm length). The different flows of lead solution (5, 7.5 and 10 mL/min) were passed through the packed bed (5, 7.5 and 10 cm) driven by a Cole Parmer MasterFlex peristaltic pump.

In all the experiments the temperature of the lead solution (60, 80 and 100 mg/L) was maintained at 40 °C. The concentration of the effluent of the column was measured at specific time intervals. The process was stopped when the saturation of the adsorbent was reached. The behavior of lead adsorption in the column, in terms of the breakthrough curve, was analyzed by the application of the Thomas, Yoon – Nelson and Dose – Reponse models.

The column capacity, q_c (mg), the adsorption capacity, q (mg/g), the percentage removal (%R) and the mass transfer zone (MTZ) were calculated in the same way as it was described in a previous study [19] using the following equations:

$$q_c = \frac{Q}{1000} \int_0^t C_{ads} \, dt$$

Where Q (mL/min) is the flow rate, C_{ads} (mg/L) is the adsorbed concentration and t (min), time.

$$q = \frac{q_c}{X}$$

Where X (g) is the mass of the adsorbent into the column.

$$\%R = \left(\frac{q_c}{m}\right)100$$

Where m (mg) is the amount of lead sent to the column at different times and is calculated by:

$$m = \frac{C_0 \cdot Q \cdot t}{100}$$

3. Results and discussion

3.1. Modeling of the batch process

3.1.1. Kinetics of adsorption process

In the batch process, where the irradiated material was used as an adsorbent, the capacity of equilibrium adsorption was reached virtually at 120 min for all concentrations at each temperature, while with the non-irradiated material, this equilibrium condition was reached at 180 min, this means that the adsorption rate is 33% faster using the irradiated material than the non-irradiated one as a lead adsorbent. Therefore, a dose of 200kGy of gamma radiation has a positive effect on the adsorption capacity of the material. This phenomenon has already been observed in previous studies at lower radiation doses [11].

Table 1 shows differences in lead removal percentages for non-irradiated and irradiated materials at various initial concentrations and temperatures. In the equilibrium time, *i.e.*, 120 min, regardless of the concentration, lead removal percentages of irradiated material were 22.34%, 26.11% and 29.59% higher than those for the non-irradiated material, obtained at 20 °C, 30 °C and 40 °C, respectively.

Table 2 shows the effect of temperature and concentration on the maximum adsorption capacity of irradiated and non-irradiated materials. The increase in the kinetic energy of the lead ions in solution due to the increase in temperature benefits the adsorption process, this

effect occurs within a range of concentrations. For the non-irradiated material, an increment of temperature from 20 °C to 40 °C represents an increase in the maximum adsorption capacity from 1.29 to 1.71 mg / g, which accounts for an increment of 33%, for 100 mg / L of concentration; while for the irradiated material, under the same conditions, such increment was of 44%. Moreover, regardless of the concentration, average increments of 27% are for the non-irradiated material and 33% for the irradiated one.

The average adsorption capacity was 1.17 for the non-irradiated material and 2.65 for the irradiated one. Thus, regardless of temperature and concentration, the adsorption capacity of the irradiated material is 2.3 times on average higher than that of the non-irritated material.

Figs. 1–6 and Tables 3–6 show the accurate fit of the experimental data of the adsorption capacity both with the pseudo-second order model and with the intraparticle diffusion model, in terms of the quadratic correlation (R^2) and the average absolute relative deviation (*AARD*). This may suggest that in the process of adsorption the phenomena of physisorption and chemisorption are involved, and in addition, that the process might be controlled by internal diffusion in virtue of the minute values of the diffusion coefficient (D $\sim 10^{-14}$ m^2/s).

Structural modifications are due to gamma irradiation, since intraparticle diffusion is favoured and the accessibility of the active sites within pores of the adsorbent is increased. Hence, the diffusion coefficient value is virtually doubled for the irradiated material. Such situation concurs with the results for the pseudo-second order kinetic model. Moreover, the adsorption capacity of the irradiated material is on average 250% greater than that for the non-irradiated.

The experimental data of the adsorption capacity were modelled with the pseudo-first order model, however the results were not satisfactory in terms of R^2 and %*AARD*, because the average values of R^2 were 0.963 for the non-irradiated material, and 0.959 for the irradiated material. In like manner, the average percentages of *AARD* were higher than 36.5% in both kind of materials.

3.1.2. Equilibrium of adsorption process

The acceptable adjustment of the experimental data with the Langmuir model in this case suggests that the adsorption of lead on the irradiated and non-irradiated material is carried out favorably ($0 < R_L < 1$), thus forming a monolayer on the surface of the adsorbent. As it is noticed in Figs. 7 and 8, as well as in Table 7, the adsorption capacity increases with the increase in temperature throughout the concentration range studied. The endothermic nature found in the kinetic study is verified by the study of the equilibrium of the adsorption process. The initial adsorption capacity (q_0) obtained with the Langmuir model is similar to the maximum capacity experimentally determined at equilibrium. The decrease of the R_L parameter and the increase of the initial adsorption capacity (q_0) with the increase in the temperature clearly show that the development of the adsorption process is much more enhanced at high temperatures. The increase of the adsorption capacity when temperature increases may be attributed to the kinetic effect, because adsorption processes, especially chemisorption, are favored when temperature increases, which raises the probability of collision between lead ions and the adsorbent, and the physicochemical interactions are carried out on its surface. Thus, the adsorbent has a greater affinity for lead ions when temperature increases. This behavior has been reported in other adsorption systems [17,21,38]. Regarding gamma radiation, once again in this case its favorable effect is evident, since the irradiated material has an adsorption capacity three times larger than the non-irradiated material.

The adsorption capacity calculated with the Dubinin – Radushkevich model is much higher than the one experimentally obtained. It is important to bear in mind that in the experimental case the former refers to the capacity of adsorption at equilibrium, while the one calculated with the D-R isotherm refers to the capacity of adsorption up

Table 1
Difference of % Removal for irradiated and non-irradiated materials.

C (mg/L)	Difference of %Removal			Difference % (regardless of temperature) (Irradiated - Nonirradiated)
	20 °C	30 °C	40 °C	
10	23.17	24.57	23.94	23.89
20	23.49	27.15	28.78	26.47
40	26.79	30.49	34.30	30.53
60	22.61	26.08	32.05	26.91
80	19.28	25.78	31.24	25.43
100	18.68	22.60	27.21	22.83
Mean	22.34	26.11	29.59	26.01

Table 2

Maximum adsorption capacity (mg/g) for irradiated and non-irradiated material.

C (mg/L)	q (mg/g) Irradiated			Mean	q (mg/g) Nonirradiated			Mean
	20 °C	30 °C	40 °C	Regardless of temperature	20 °C	30 °C	40 °C	Regardless of temperature
10	0.764	0.833	0.867	0.821	0.553	0.603	0.643	0.600
20	1.364	1.530	1.629	1.508	0.811	0.930	1.019	0.920
40	2.218	2.619	2.879	2.572	1.085	1.245	1.314	1.215
60	2.661	3.218	3.898	3.259	1.160	1.390	1.519	1.356
80	2.971	3.714	4.325	3.670	1.262	1.476	1.589	1.442
100	3.332	4.012	4.808	4.051	1.286	1.512	1.713	1.504
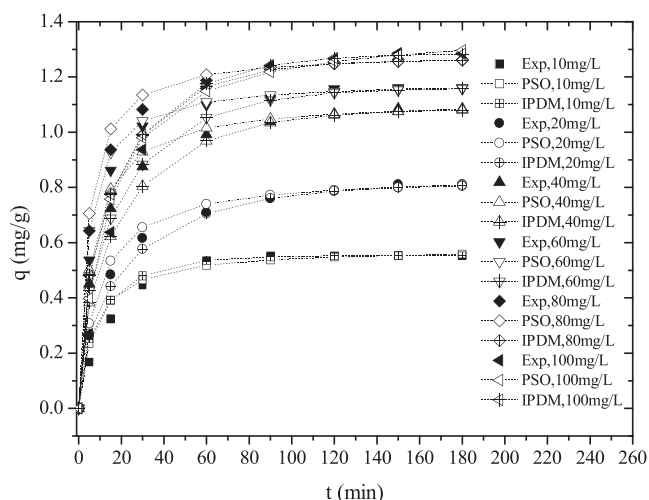
Fig. 1. Adsorption capacity, experimental and calculated with the kinetic models of Pseudo-Second Order (PSOM) and Intraparticle Diffusion Model (IPDM) at 20 °C for the non-irradiated material.
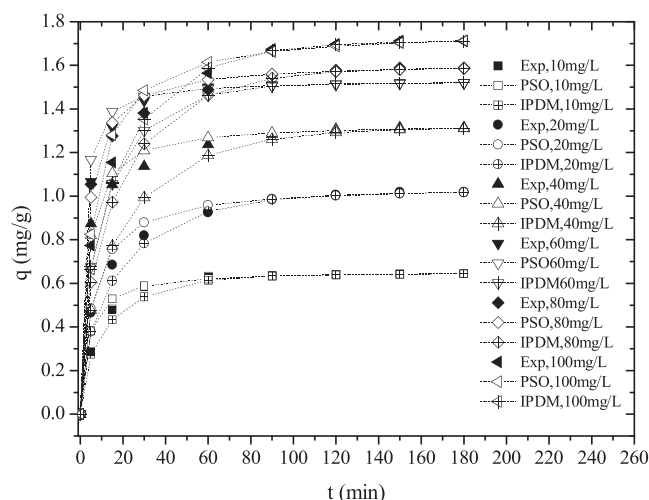
Fig. 3. Adsorption capacity, experimental and calculated with the kinetic models of Pseudo-Second Order (PSO) and Intraparticle Diffusion Model (IPDM) at 40 °C for the non-irradiated material.
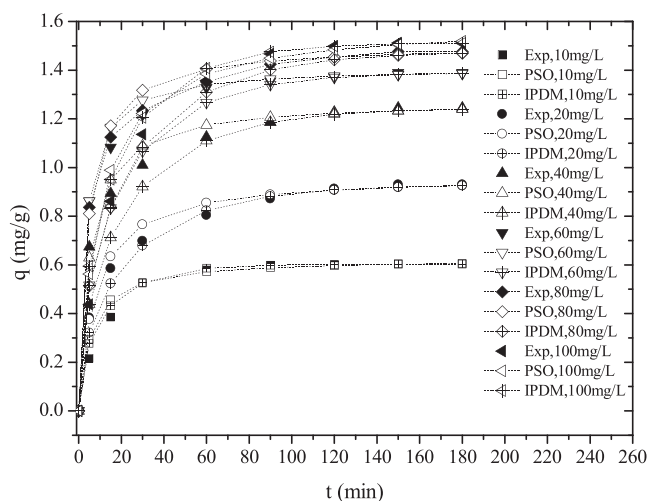
Fig. 2. Adsorption capacity, experimental and calculated with the kinetic models of Pseudo-Second Order (PSO) and Intraparticle Diffusion Model (IPDM) at 30 °C for the non-irradiated material.
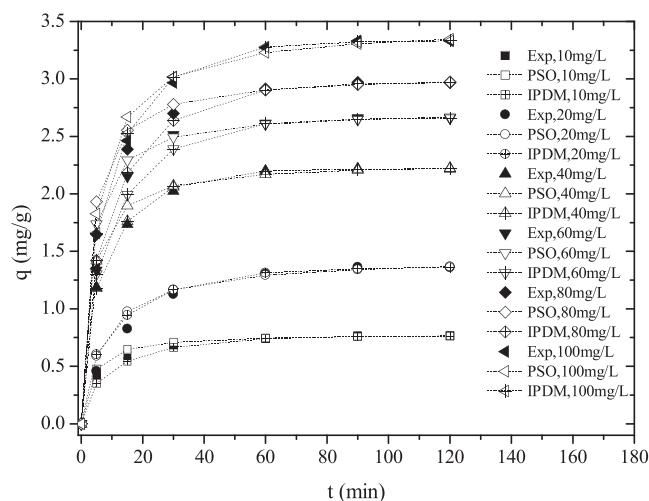

Fig. 4. Adsorption capacity, experimental and calculated with the kinetic models of Pseudo-Second Order (PSO) and Intraparticle Diffusion Model (IPDM) at 20 °C for the irradiated material.

to saturation. However, as it is displayed in Table 8, according to the value of the mean free energy ($E > 10$ kJ/mol), the phenomenon that occurs in the process of adsorption of lead on irradiated and non-irradiated materials is chemisorption rather than physisorption.

The deviation of the values of the adsorption capacity calculated with the two isotherms with regards to the experimental values are shown in Figs. 9 and 10, and in Tables 7 and 8; a better fit is found for the non-irradiated material than for the irradiated material.

As can be seen in Table 9, the maximum adsorption capacity of this

irradiated material is higher than that of some biosorbents, but it is similar to that shown by activated carbon obtained from different natural sources.

3.1.3. Thermodynamics of the adsorption process

The thermodynamic parameters of the adsorption process were evaluated. The change in free energy was obtained from the adsorption constant. Since the effect of the temperature is positive, the value of K_{ads} increases with temperature, this effect is more favorable at low
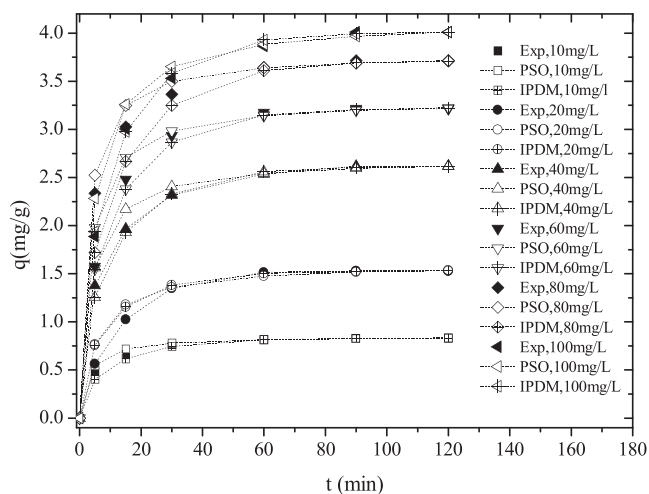
Fig. 5. Adsorption capacity, experimental and calculated with the kinetic models of Pseudo-Second Order (PSO) and Intraparticle Diffusion Model (IPDM) at 30 °C for the irradiated material.

Fig. 6. Adsorption capacity, experimental and calculated with the kinetic models of Pseudo-Second Order (PSO) and Intraparticle Diffusion Model (IPDM) at 40 °C for the irradiated material.
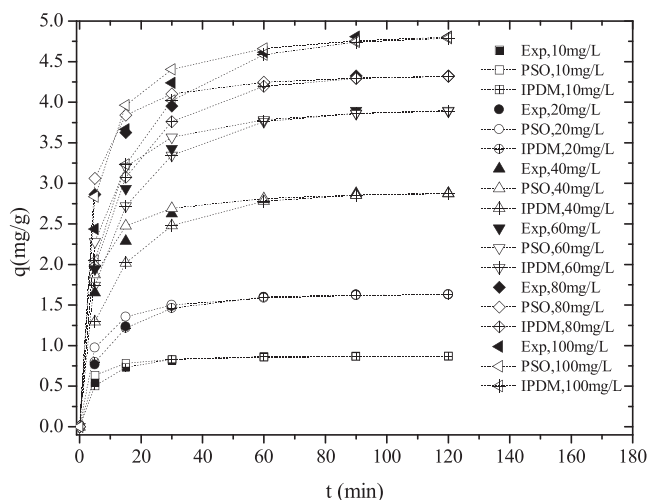
Table 3
Parameters of the kinetic model of Pseudo-Second Order for the process of adsorption of lead in the non-irradiated material.

Pseudo-Second Order					
C_0(mg/L)	T(°C)	q_e (mg/g)	k_2(g/mg·min)	R^2	AARD(%)
10	20	0.581	0.235	0.9967	8.097
	30	0.625	0.286	0.9982	6.507
	40	0.658	0.423	0.9992	5.203
20	20	0.848	0.134	0.9967	4.539
	30	0.966	0.132	0.9991	3.389
	40	1.051	0.163	0.9992	2.963
40	20	1.120	0.015	0.9985	3.483
	30	1.275	0.153	0.9986	3.177
	40	1.335	0.239	0.9995	2.391
60	20	1.188	0.199	0.9992	3.628
	30	1.412	0.222	0.9995	1.651
	40	1.533	0.417	0.9999	1.911
80	20	1.291	0.187	0.9993	2.797
	30	1.506	0.155	0.9991	2.219
	40	1.614	0.199	0.9995	2.287
100	20	1.386	0.058	0.9926	8.413
	30	1.597	0.068	0.9963	6.242
	40	1.768	0.099	0.9985	3.320

Table 4
Parameters of the kinetic model of Pseudo-Second Order for the process of adsorption of lead in the irradiated material.

Pseudo-Second Order					
C_0(mg/L)	T(°C)	q_e (mg/g)	k_2(g/mg·min)	R^2	AARD(%)
10	20	0.785	0.391	0.9987	3.773
	30	0.853	0.417	0.9991	3.721
	40	0.883	0.586	0.9994	3.718
20	20	1.451	0.094	0.9937	7.549
	30	1.611	0.113	0.9954	8.056
	40	1.683	0.163	0.9982	5.617
40	20	2.281	0.144	0.9987	4.761
	30	2.698	0.102	0.9983	4.133
	40	2.947	0.119	0.9991	3.655
60	20	2.731	0.128	0.9988	5.512
	30	3.319	0.089	0.9984	5.474
	40	4.023	0.065	0.9982	4.534
80	20	3.045	0.114	0.9991	4.029
	30	3.792	0.105	0.9992	2.895
	40	4.401	0.104	0.9994	2.523
100	20	3.471	0.064	0.9971	6.877
	30	4.148	0.059	0.9981	4.910
	40	4.953	0.054	0.9980	4.361

concentrations, as observed in Tables 10 and 11. The value of the K_{ads} in the irradiated adsorbent is virtually twice as much as of the non-irradiated adsorbent.

The negative value in the free energy change indicates the spontaneity of the adsorption process. The spontaneity of the process increases with temperature, this phenomenon is more evident in the irradiated adsorbent.

As it is evident, the endothermic nature of the adsorption process is confirmed by the positive value in enthalpy change. This energy requirement, necessary for the adsorption of lead to take place, is greater in the irradiated adsorbent than in the non-irradiated adsorbent. A positive value in enthalpy change also indicates that the lead was chemisorbed, because physisorption is always exothermic [49].

The positive value in entropy change suggests that there is good affinity of the lead ions on the adsorbent, of course, this affinity is greater at low concentrations; in such case, the process may be irreversible.

The positive value of isosteric heat confirms that the process is endothermic. Isosteric heat also indicates that in the adsorption process there is an energetically heterogeneous interaction between the lead ions and the adsorbent. This interaction is stronger at lower

concentrations and with the irradiated adsorbent.

As it is noticed in Table 12, the comparison of each one of the values of the parameters and properties is advantageous for the irradiated adsorbent. For instance, the time to reach equilibrium was reduced 33%, adsorption capacity increased in 180%, the average diffusion coefficient was virtually doubled.

In addition, the spontaneity and endothermicity of the process were also improved, as well as the affinity of the lead with the irradiated mineral. Also, the covered surface of the adsorbent was increased, which is evinced in the comparison of the value of the adsorption constant.

Therefore, experimentation in the continuous process will only be carried out using the irradiated material as adsorbent.

### 3.2. Modeling of the continuous process

The experimental results of lead adsorption in the column operated in continuous process are presented in Table 13. The effect of three flow rates (5, 7.5 and 10 mL/min), three bed heights (5, 7.5 and 10 cm) with

Table 5

Parameters of the Intraparticle-Diffusion Model for the process of adsorption of lead in the non-irradiated material.

Intraparticle-Diffusion Model				
C_0(mg/L)	T(°C)	$D \times 10^{14}$ (m²/s)	R^2	AARD(%)
10	20	1.914	0.9928	10.065
	30	1.955	0.9976	5.164
	40	1.645	0.9776	3.186
20	20	0.959	0.9967	2.634
	30	1.037	0.9801	4.377
	40	1.216	0.9965	4.463
40	20	1.086	0.9962	5.234
	30	1.077	0.9844	8.479
	40	1.151	0.9960	10.587
60	20	1.179	0.9785	7.649
	30	1.212	0.9813	10.268
	40	1.796	0.9786	8.627
80	20	1.298	0.9970	6.714
	30	1.053	0.9944	10.440
	40	1.277	0.9919	10.066
100	20	1.228	0.9988	10.600
	30	1.371	0.9938	7.170
	40	1.330	0.9941	3.316

Table 6

Parameters of the Intraparticle-Diffusion Model for the process of adsorption of lead in the irradiated material.

Intraparticle-Diffusion Model				
C_0(mg/L)	T(°C)	$D \times 10^{14}$ (m²/s)	R^2	AARD(%)
10	20	2.462	0.9928	10.410
	30	2.693	0.9916	8.188
	40	2.588	0.9719	2.217
20	20	2.289	0.9984	8.570
	30	2.951	0.9988	8.462
	40	2.861	0.9959	1.273
40	20	3.481	0.9962	1.668
	30	2.741	0.9883	2.168
	40	2.368	0.9890	6.804
60	20	2.882	0.9816	2.530
	30	2.767	0.9956	1.581
	40	2.336	0.9980	3.614
80	20	2.720	0.9973	4.266
	30	2.536	0.983	7.231
	40	2.468	0.9962	8.801
100	20	2.993	0.9995	4.632
	30	2.793	0.9980	1.228
	40	2.105	0.9901	5.879
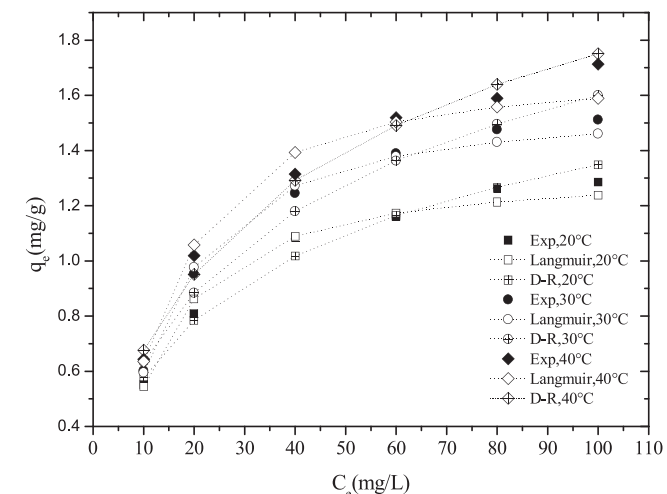
Fig. 7. Adsorption isotherms at 20, 30 and 40 °C of the non-irradiated material.
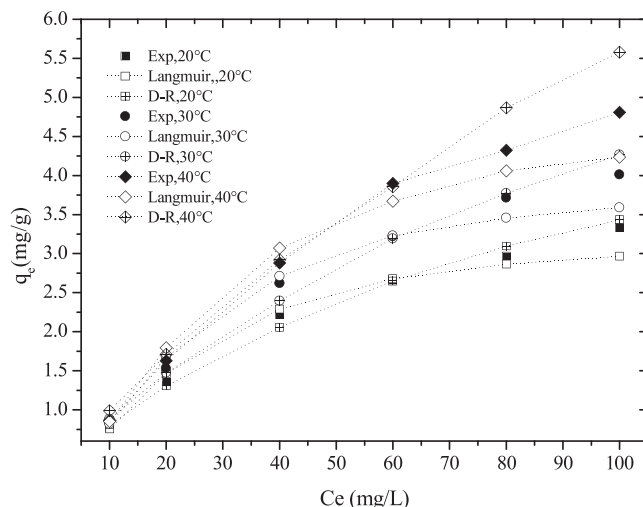
Fig. 8. Adsorption isotherms at 20, 30 and 40 °C of the irradiated material.

Table 7

Parameters of the Langmuir Isotherm.

Langmuir Isotherm						
Mineral	T(°C)	q_0(mg/g)	K_L (L/mg)	R_L	R^2	AARD(%)
Non-irradiated	20	1.330	0.152	0.137	0.9900	2.795
	30	1.585	0.155	0.136	0.9976	2.173
	40	1.704	0.167	0.129	0.9915	3.521
Irradiated 200kGy	20	3.325	0.124	0.156	0.9936	4.579
	30	3.976	0.155	0.136	0.9927	5.374
	40	6.032	0.227	0.105	0.9972	7.118

their corresponding mass of adsorbent (17.136, 25.703 and 34.271 g) and three initial concentrations (60, 80 and 100 mg/L) on the adsorption capacity of the column (q_{column}), the mass transfer zone (MTZ), the service time or breakthrough time (t_b), the percentage of lead removal (%R) and the treated volume (V) were studied.

The graphical representation of the continuous behavior of the process of adsorption of lead in the irradiated material is shown in Figs. 11–13. It can be seen that the shape is like an ideal "S". This type "S" behavior is representative in adsorbents of small particle size [50].

3.2.1. Effect of flow rate

The breaking curves at three different flow rates are shown in Fig. 11. In this case, the height of the packed bed was 10 cm and the lead concentration was 100 mg/L. The variation in the flow rate impacts contact time. At lower flow rates, contact time is longer, therefore, breaking time increases, the capacity of the column is larger, the removal rate is also higher, and the treated volume is the highest, as it is displayed in Table 10.

An increase in the flow rate from 5 to 10 mL/min not only modifies the speed of adsorption, also the capacity of adsorption of the column decreases by 13%. The breakthrough time decreases by 58%, the removal process decreases 20.7% and the treated volume decreases 16.5%. This is because lead saturates the adsorbent material faster, which is seen with an increase in the slope of the curves and an increase in the height of the mass transfer zone.
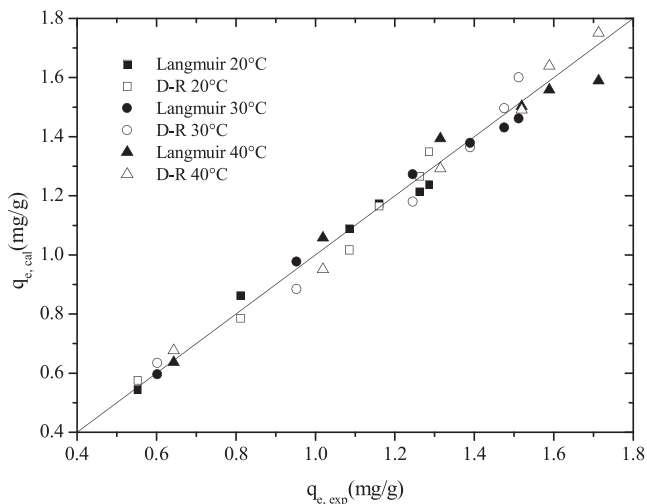
3.2.2. Effect of bed height

Fig. 12 shows the effect of bed height (5, 7.5 and 10 cm) on breakthrough time. As it is seen, the higher the packed bed, the longer the breakthrough time. Obviously, this has a favorable effect on the adsorption capacity of the column and on the treated volume.

Table 8
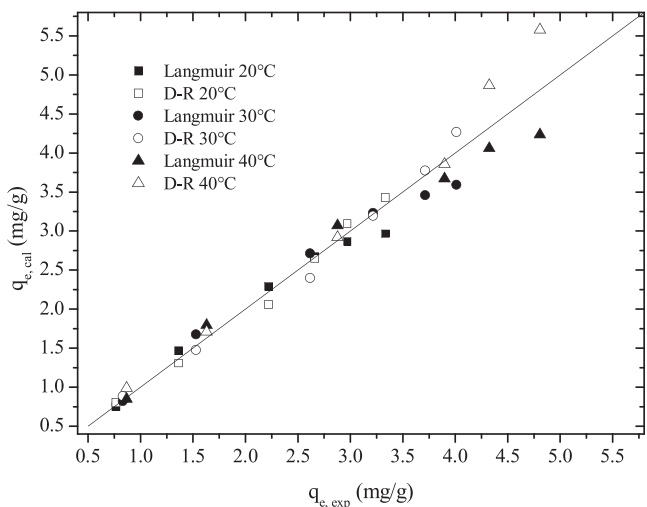Parameters of the Dubinin–Radushkevich Isotherm.

Dubinin – Radushkevich Isotherm Mineral	T(°C)	q_s(mg/g)	$K_{ads} \times 10^6$ (mol^2/kJ^2)	E(kJ/mol)	R^2	AARD(%)
Non-irradiated	20	3.443	2.609	13.843	0.983	3.213
	30	4.239	2.517	14.094	0.9751	4.472
	40	4.690	2.374	14.512	0.9861	3.476
Irradiated 200kGy	20	14.522	3.756	11.538	0.9917	4.113
	30	18.594	3.489	11.971	0.9909	4.505
	40	34.631	3.330	12.253	0.9798	8.310

Fig. 9. Comparison of the experimental and calculated adsorption capacity with the Langmuir and Dubinin – Radushkevich isotherms at 20, 30 and 40 °C of the non-irradiated material.

Fig. 10. Comparison of the experimental and calculated adsorption capacity with the Langmuir and Dubinin – Radushkevich isotherms at 20, 30 and 40 °C of the irradiated material.

3.2.3. Effect of initial concentration

The effect of the initial concentration on breakthrough time is shown in Fig. 13. By increasing the initial concentration, the service time of the column decreases. This produces a smaller treated volume; however, the adsorption capacity of the column and the percentage of removal of lead increase. When the initial concentration is increased

Table 9
Comparison of calculated adsorption capacity of gamma irradiated Calcite and Calcite employing different organic and inorganic adsorbents.

Adsorbent	C_0 (mg/L)	q (mg/g)	Reference
Gamma irradiation	100	34.631	This study
Activated Carbon from waster rubber tire	100	1.42	Rao et al. [39]
Moringa oleifera seed powder	50	3.30	Kowanga et al. [40]
	100	6.46	
Activated Carbon from hazelnut husk	200	13.05	Imamoglu and Tekir [41]
Carbon nanotubes	2	15.34	Mubarak et al. [42]
Calcium Alginate Beads	100	15.921	Alfaro-Cuevas-Villanueva et al. [17]
Activated carbon from plantain peels	100	28.11	Inam et al. [43]
Activated carbon cashew nut shells	40	28.9	Tangjuank et al. [44]
Turkish kaolinite clay	400	31.75	Sari et al. [45]
Lignin from *Hagenia Abyssinica*	100	41	Tesfaw et al. [46]
Bentonite clay	1300	51.9	Al Jlil [47]
Cr-pillared clays	200	222.22	Georgescu et al. [48]
Aminofunctionalized silica monolith	89.5	450	Sharififard et al. [14]

from 60 to 100 mg/L, in spite that the service time of the column and the treated volume decrease by 43%, the adsorption capacity of the column increases 84% and the percentage of removal of lead increases 55%. This way, even though the adsorbent saturates faster, the amount of lead removed is greater.

3.2.4. Modeling of breakthrough curves

As it is displayed in Table 14, the fit of the experimental data with the Thomas, Dose – Reponse and Yoon – Nelson models is satisfactory in terms of the quadratic correlation coefficient.

In the case of the adjustment with the Thomas model, a maximum adsorption capacity of 5.122 mg/g was obtained. The effect of the initial concentration is evident, as the initial concentration increases from 60 to 100 mg/L, while the adsorption capacity increases 23%.

Moreover, in the case of the Dose – Reponse model, the variable with a positive effect on the capacity of adsorption was the height of the packed bed. The adsorption capacity increased 168% when the packed bed height was doubled.

With the Yoon – Nelson model, the time to adsorb half of the lead fed to the column doubles with the half-rate decrease in flow.

4. Conclusions

Equilibrium time decreases from 180 min to 120 min; this is to say, it is reduced 33% with the irradiated material.

Regardless of the concentration and temperature, 26% more lead is removed by the irradiated material than that by the non-irradiated one, since the adsorption capacity of the irradiated material is 2.3 times on average higher than that of the non-irradiated.

The experimental results of the kinetics of the adsorption process were satisfactorily adjusted with the pseudo-second order model, with an AARD of 4.01% for the non-irradiated material and 4.78% for the irradiated mineral. With the intraparticle diffusion model, the AARD value was 7.17% and 4.97% for the non-irradiated and irradiated material, respectively.

The diffusion coefficient increases 135% on average in the irradiated material with regards to the diffusion coefficient in the non-irradiated material.

The adsorption process was successfully adjusted with the models of the adsorption isotherms of Langmuir and Dubinin – Radushkevich. From the results of the parameters of the Langmuir isotherm, it was obtained that the adsorption process is favorable, that is, it had a

Table 10
Thermodynamic parameters of the lead adsorption process in the non-irradiated material.

C_0 (mg/L)	T(°C)	K_{ads}	$\Delta G°$ (KJ/mol)	$\Delta H°$ (KJ/mol)	$\Delta S°$ (KJ/mol K)	ΔH_{st} (KJ/mol)
10	20	123.464	−11.738	14.451	0.089	8.644
	30	151.446	−12.653			
	40	180.269	−13.524			
20	20	68.237	−10.292	16.077	0.089	7.337
	30	89.082	−11.315			
	40	103.874	−12.089			
40	20	37.212	−8.815	10.501	0.066	3.142
	30	45.201	−9.606			
	40	48.943	−10.129			
60	20	37.212	−7.743	13.262	0.072	2.947
	30	45.201	−8.584			
	40	48.943	−9.174			
80	20	37.212	−7.142	10.708	0.061	1.900
	30	45.201	−7.861			
	40	48.943	−8.358			
100	20	37.212	−6.561	12.870	0.066	1.918
	30	45.201	−7.259			
	40	48.943	−7.885			

Table 11
Thermodynamic parameters of the lead adsorption process in the irradiated material.

| C_0 (mg/L)	T(°C)	K_{ads}	$\Delta G°$ (KJ/mol)	$\Delta H°$ (KJ/mol)	$\Delta S°$ (KJ/molK)	ΔH_{st} (KJ/mol)
10	20	324.088	−14.090	26.790	0.140	21.948
	30	497.015	−15.648			
	40	653.012	−16.875			
20	20	214.268	−13.081	27.420	0.138	20.614
	30	325.894	−14.584			
	40	439.084	−15.842			
40	20	124.517	−11.7584	27.656	0.135	17.686
	30	189.687	−13.2204			
	40	256.761	−14.4448			
60	20	79.695	−10.671	32.181	0.146	17.617
	30	115.703	−11.974			
	40	185.470	−13.598			
80	20	59.084	−9.941	26.315	0.124	11.965
	30	86.672	−11.246			
	40	117.675	−12.413			
100	20	49.970	−9.533	23.521	0.113	9.53
	30	67.001	−10.597			
	40	92.604	−11.790			

Table 12
Comparison of the parameters and properties of lead adsorption in the non-irradiated and irradiated material in the batch process.

| Parameter or Property	Non-irradiated	Irradiated
Equilibrium Time (min)	180	120
Maximum Adsorption Capacity (mg/g)		
Experimental	1.713	4.808
Langmuir Isotherm	1.704	6.032
Dubinin – Radushkevich Isotherm	4.690	34.631
Pseudo-Second Order	1.768	4.953
Average Diffusion Coefficient (m²/s)	1.32×10^{-14}	2.67×10^{-14}
Average Thermodynamic Properties		
K_{ads}	68.99	215.455
$\Delta G°$ (KJ/mol)	−9.485	−12.850
$\Delta H°$ (KJ/mol)	12.978	27.314
$\Delta S°$ (KJ/mol K)	0.074	0.133
ΔH_{st} (KJ/mol)	4.315	16.560

maximum adsorption capacity covered by a monolayer of 1.54 mg/g on average for the non-irradiated material, and 4.44 mg/g for the irradiated material. With the results of the parameters of the Dubinin –

Table 13
Experimental parameters of lead adsorption in column.

Q (mL/min)	Z (cm)	C_0 (mg/L)	q_{column} (mg/g)	X (g)	MTZ (cm)	t_b (min)	% R	V (mL)
5	10	100	4.602	34.271	5.692	232.65	86.98	1163.25
7.5	10	100	4.086	34.271	6.833	123.50	75.57	926.27
10	10	100	3.998	34.271	6.865	97.17	69.00	971.71
5	7.5	100	4.089	25.703	4.085	64.05	76.46	320.27
5	5	100	3.938	17.136	5.567	121.15	75.07	605.77
5	10	80	3.759	34.271	4.311	324.29	72.17	1621.45
5	10	60	2.494	34.271	3.150	411.02	56.15	2055.08
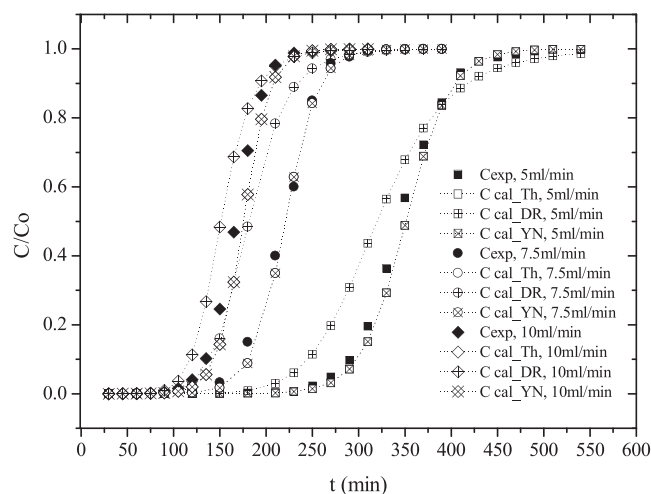
Fig. 11. Breakthrough curves at different flow rates (Z = 10 cm, C_0 = 100 mg/ L).
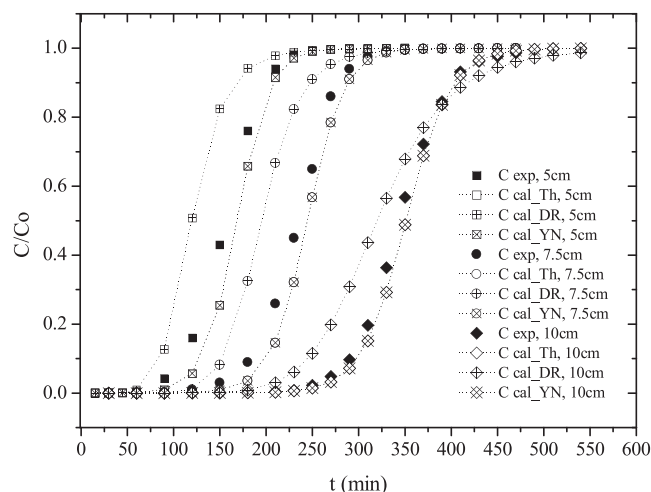
Fig. 12. Breakthrough curves at different bed heights (Q = 5 mL/min, C_0 = 100 mg/L).

Radushkevich isotherm, it can be inferred that it is a chemisorption process ($E > 10$ kJ / mol) with a theoretical adsorption capacity of 4.124 mg/g and 22.582 mg/g for the material not irradiated and irradiated, respectively.

The process in which the irradiated material is used is more spontaneous; therefore, it presents values of distribution coefficient, enthalpy, entropy, isosteric heat of adsorption greater than the adsorption process with the non-irradiated material.

The highest adsorption capacity in the continuous process (4.602 mg/g) was achieved at 40 °C, with a 100 mg/L lead initial concentration solution, within a flow rate of 5 mL/min and a bed depth of
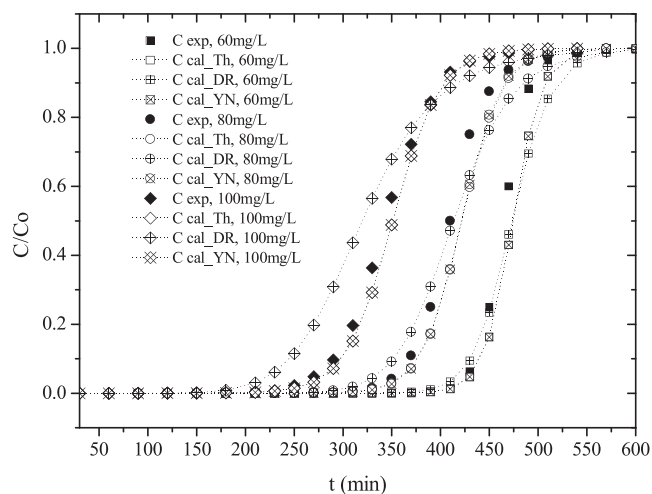
Fig. 13. Breakthrough curves at different initial concentrations (Q = 5 mL/min, Z = 10 cm).

Table 14
Parameters of the models in continuous process.

Model	Q(mL/min)	Z(cm)	C_0(mg/L)	q_0(mg/g)	K_{Th}(mL/min mg)	R^2
Thomas	5	10	100	5.122	0.419	0.9875
	7.5	10	100	4.833	0.573	0.9861
	10	10	100	5.122	0.700	0.9778
	5	7.5	100	4.759	0.510	0.9667
	5	5	100	4.921	0.576	0.9739
	5	10	80	4.925	0.612	0.9925
	5	10	60	4.151	0.973	0.9937

Model	Q(mL/min)	Z(cm)	C_0(mg/L)	q_0(mg/g)	a	R^2
Dose – Reponse	5	10	100	4.665	8.279	0.9306
	7.5	10	100	3.968	8.752	0.9457
	10	10	100	4.409	8.953	0.9641
	5	7.5	100	2.841	9.266	0.9572
	5	5	100	1.742	6.782	0.9562
	5	10	80	4.826	13.783	0.9697
	5	10	60	4.142	23.598	0.9687

Model	Q(mL/min)	Z(cm)	C_0(mg/L)	τ(min)	K_{Y-N}(min^{-1})	R^2
Yoon – Nelson	5	10	100	351.100	0.0419	0.9875
	7.5	10	100	220.840	0.0573	0.9861
	10	10	100	175.530	0.0700	0.9778
	5	7.5	100	244.670	0.0510	0.9667
	5	5	100	168.660	0.0576	0.9739
	5	10	80	421.470	0.0502	0.9911
	5	10	60	474.160	0.0678	0.9937

10 cm. The breakthrough time for a lead concentration at the exit of the column equal to 1 mg/L was 232.65 min. In this case, the effective mass transfer zone (MTZ) in packed bed was 5.7 cm for a treated volume of 1163.25 mL and a lead removal of 86.98%. The column experimental results, in terms of the breakthrough curve, were better fitted with the Thomas and Yoon – Nelson models than with the Dose – Reponse model.

References

[1] Ph.J. Landrigan, C.B. Schechter, J.M. Lipton, M.C. Fahs, J. Schwartz, Environmental pollutants and disease in American children: estimates of morbidity, mortality, and costs for lead poisoning, asthma, cancer, and developmental disabilities, Environ. Health Perspect. 110 (7) (2002) 721–728.

[2] A. Navas-Acien, E. Guallar, E.K. Silbergeld, S.J. Rothenberg, Lead exposure and cardiovascular disease-a systematic review, Environ. Health Perspect. 115 (3) (2007) 472–482.

[3] L. Järup, Hazards of heavy metal contamination, Br. Med. Bull. 68 (2003) 167–182.

[4] P. Karrari, O. Mehrpour, M. Abdollahi, A systematic review on status of lead pollution and toxicity in Iran; guidance for preventive measures, Daru J. Pharm. Sci. 20 (2) (2012) 2–17.

[5] I. Ali, V.K. Gupta, Advances in water treatment by adsorption technology, Nat. Protoc. 1 (6) (2006) 2661–2667.

[6] D.I. Caviedes Rubio, R.A. Muñoz Calderón, A. Perdomo Gualtero, D. Rodríguez Acosta, I.J. Sandoval Rojas, Treatments for removal of heavy metals commonly found in industrial wastewater. A review, Revista Ingeniería y Región 13 (1) (2015) 73–90.

[7] J. Cruz-Olivares, C. Pérez-Alonso, C. Barrera-Díaz, G. López, P. Balderas-Hernández, Inside the removal of lead (II) from aqueous solutions by De-Oiled Allspice Husk in batch and continuous processes, J. Hazard. Mater. 181 (1) (2010) 1095–1101.

[8] E. Palma-Anaya, Ch. Fall, T. Torres-Blancas, P. Balderas-Hernández, J. Cruz-Olivares, C.E. Barrera-Díaz, G. Roa-Morales, Pb(II) removal process in a packed column system with xanthation-modified deoiled allspice husk, J. Chem. 2017 (2017) 1–8.

[9] D. Mohan, A. Sarswat, Y. Sik Ok, Ch.U. Pittman Jr., Organic and inorganic contaminants removal from water with biochar, a renewable, low cost and sustainable adsorbent – a critical review, Bioresour. Technol. 160 (2014) 191–202.

[10] M.J. Amiri, J. Abedi-Koupai, S.S. Eslamian, M. Arshadi, Adsorption of Pb(II) and Hg (II) ions from aqueous single metal solutions by using surfactant-modified ostrich bone waste, Desalin. Water Treat. 57 (2016) 16522–16539.

[11] J. Cruz-Olivares, G. Martínez-Barrera, C. Pérez-Alonso, C.E. Barrera-Díaz, M.C. Chaparro-Mercado, F. Ureña-Núñez, Adsorption of lead ions from aqueous solutions using gamma irradiated minerals, J. Chem. 2016 (2016) 1–7.

[12] S.M. Shaheen, A.S. Derbalah, F.S. Moghanm, Removal of heavy metals from aqueous solution by zeolite in competitive sorption system, Int. J. Environ. Sci. Dev. 3 (4) (2012) 362–367.

[13] S.U. Khan, I.H. Farooqi, S. Ayub, Studies on application of Fe based binary oxide nanoparticles for treatment of lead (Pb 2+) contaminated water-a batch study, Mater. Today Proc. 4 (9) (2017) 9650–9655.

[14] H. Sharififard, P. Aprea, D. Caputo, F. Pepe, Aminofunctionalized silica monolith for Pb2+ removal: synthesis and adsorption experiments, Desalin. Water Treat. 105 (2018) 287–297.

[15] D.M. Gore, I. Snape, 50 kGy of gamma irradiation does not affect the leachability of mineral soils and sediments, Powder Diffr. 29 (2014) 40–46.

[16] J. Cruz-Olivares, C. Pérez-Alonso, C. Barrera-Díaz, R. Natividad, M.C. Chaparro-Mercado, Thermodynamical and analytical evidence of lead ions chemisorption onto Pimenta dioica, Chem. Eng. J. 166 (3) (2011) 814–821.

[17] R. Alfaro-Cuevas-Villanueva, A.R. Hidalgo-Vázquez, C.J. Cortés Penagos, R. Cortés-Martínez, Thermodynamic, kinetic, and equilibrium parameters for the removal of lead and cadmium from aqueous solutions with calcium alginate beads, Sci. World J. 2014 (2014) 1–9.

[18] D. Ghahremani, I. Mobasherpour, S.A. Mirhosseini, Sorption thermodynamic and kinetic studies of Lead removal from aqueous solutions by nano Tricalcium phosphate, ulletin de la Société Royale des sciences de Liège 86 (2017) 96–112.

[19] J. Cruz-Olivares, C. Pérez-Alonso, C. Barrera-Díaz, F. Ureña-Nuñez, M.C. Chaparro-Mercado, B. Bilyeu, Modeling of lead (II) biosorption by residue of allspice in a fixed-bed column, Chem. Eng. J. 228 (2013) 21–27.

[20] M.G.A. Vieira, A.F. de Almeida Neto, M.G.C. da Silva, C.N. Carneiro, A.A. Melo Filho, Adsorption of lead and copper ions from aqueous effluents on rice husk ash in a dynamic system, Braz. J. Chem. Eng. 31 (02) (2014) 519–529.

[21] A.O. Dada, A.P. Olalekan, A.M. Olatunya, O. Dada, Langmuir, Freundlich, Temkin and Dubinin–Radushkevich Isotherms Studies of Equilibrium Sorption of Zn^{2+} Unto Phosphoric Acid Modified Rice Husk, IOSR J. Appl. Chem. 3 (1) (2012) 38–45.

[22] X. Chen, Modeling of experimental adsorption isotherm data, Information 6 (2015) 14–22.

[23] J. He, S. Hong, L. Zhang, F. Gan, Y.-S. Ho, Equilibrium and thermodynamic parameters of adsorption of methylene blue onto rectorite, Fresenius Environ.Bull. 19 (11a) (2010) 2651–2656.

[24] D. Figueroa, A. Moreno, A. Hormaza, Equilibrio, termodinámica y modelos cinéticos en la adsorción de Rojo 40 sobre tuza de maíz, Revista Ingenierías Universidad de Medellín 14 (26) (2015) 105–120.

[25] Wua F-Ch, Tsengb R-L, Juang R-S, Characteristics of Elovich equation used for the analysis of adsorption kinetics in dye-chitosan systems, Chem. Eng. J. 150 (2009) 366–373.

[26] S.M. Yakout, E. Elsherif, Batch kinetics, isotherm and thermodynamic studies of adsorption of strontium from aqueous solutions onto low cost rice-straw based carbons, Carbon – Sci. Technol. 1 (2010) 144–153.

[27] N. Bhadusha, T. Ananthabaskaran, Kinetic, thermodynamic and equilibrium studies on uptake of rhodamine B onto ZnCl2 activated low cost carbon, E-J. Chem. 9 (1) (2012) 137–144.

[28] L. Largitte, P. Lodewyckx, Kinetics and thermodynamics of the adsorption of lead (II) on an activated carbon from coconut shells, Eurasian Chem. J. 15 (2013) 283–292.

[29] S.M. Silva, K.A. Sampaio, R. Ceriani, R. Verhé, C. Stevens, W. De Greyt, A.J.A. Meirelles, Adsorption of carotenes and phosphorus from palm oil onto acid activated bleaching earth: equilibrium, kinetics and thermodynamics, J. Food Eng. 118 (4) (2013) 341–349.

[30] V.C. Taty-Costodes, H. Fauduet, C. Porte, Y.S. Ho, Removal of lead (II) ions from synthetic and real effluents using immobilized Pinus sylvestris sawdust: adsorption on a fixed-bed column, J. Hazard. Mater. B123 (2005) 135–144.

[31] P.D. Rocha, A.S. Franca, L.S. Oliveira, Batch and column studies of phenol adsorption by an activated carbon based on acid treatment of corn cobs, IACSIT Int. J. Eng. Technol. 7 (6) (2015) 1–6.

[32] M.A. Mahmoud, Kinetics studies of uranium sorption by powdered corn cob in

batch and fixed bed system, J. Adv. Res. 7 (2016) 79–87.

[33] A.B. Albadarin, Ch. Mangwandi, A.H. Al-Muhtaseb, G.M. Walker, S.J. Allen, M.N.M. Ahmad, Modelling and fixed bed column adsorption of Cr(VI) onto ortho-phosphoric acid-activated lignin, Chin. J. Chem. Eng. 20 (3) (2012) 469–477.

[34] A.W.W.A. APHA, Standard Methods for the Examination of Water and Wastewater, 19th ed., American Public Health Association, Washington, DC, 1995.

[35] L. Zheng, Z. Dang, X. Yi, H. Zhang, Equilibrium and kinetics studies of adsorption of Cd(II) from aqueous solution using modified corn stalk, J. Hazard. Mater. 176 (1-2) (2010) 650–656.

[36] K. Urano, H. Tachikawa, Process development for removal and recovery of phosphorus from wastewater by new adsorbent. Adsorption rates and breakthrough curves, Ind. Eng. Chem. Res. 30 (1991) 1897–1899.

[37] D.D. Do, Adsorption Analysis, Equilibria and Kinetics, London, 1998.

[38] A. Mittal, L. Kurup, J. Mittal, Freundlich and Langmuir adsorption isotherms and kinetics for the removal of Tartrazine from aqueous solutions using hen feathers, J. Hazard. Mater. 146 (2007) 243–248.

[39] H.J. Rao, P. King, Y.P. Kumar, Experimental investigation on adsorption of lead from aqueous solution using activated carbon from the waste rubber tire: optimization of process parameters using central composite design, Rasayan J. Chem. 9 (2) (2016) 254–277.

[40] K.D. Kowanga, E. Gatabe, G.O. Mauti, E.M. Mauti, Kinetic, sorption isotherms, pseudo-first-order model and peudo-second-order model studies of Cu(II) and Pb(II) using defatted Moringa oleifera seed powder, J. Phytopharmacol. 5 (2) (2016) 71–78.

[41] M. Imamoglu, O. Tekir, Removal of copper (II) and lead (II) ions from aqueous solutions by adsorption on activated carbon from a new precursor hazelnut husks, Desalination 228 (2008) 108–113.

[42] N.M. Mubarak, M. Thobashinni, E.C. Abdullah, J.N. Sahu, Comparative kinetic study of removal of Pb2+ ions and Cr3+ ions from waste water using carbon nanotubes produced using microwave heating, J. Carbon Res. 2 (7) (2016) 1–16.

[43] E.I. Inam, U.J. Etim, E.G. Akpabio, S.A. Umoren, Simultaneous adsorption of lead (II) and 3,7-Bis(dimethylamino)-phenothiazin-5-ium chloride from aqueous solution by activated carbon prepared from plantain peels, Desalin. Water Treat. 1 (2015) 1–14.

[44] S. Tangjuank, N. Insuk, J. Tontrakoon, V. Udeye, Adsorption of lead(II) and cadmium(II) ions from aqueous solutions by adsorption on activated carbon prepared from cashew nut shella, Int. J. Chem. Mol. Eng. 3 (4) (2009) 221–227.

[45] A. Sari, M. Tuzen, D. Citak, M. Soylak, Equilibrium kinetic and thermodynamic studies of adsorption of Pb(II) from aqueous solutions onto Turkish kaolinite clay, J. Hazard. Mater. 149 (2007) 283–291.

[46] B. Tesfaw, F. Chekol, S. Mehretie, S. Admassie, Adsorption of Pb(II) ions from aqueous solution using lignin from Hagenia Abyssinica, Bull. Chem. Soc. Ethiop. 30 (3) (2016) 473–484.

[47] S. Al-Jlil, Kinetics of adsorption of chromium and lead ions on bentonite clay using novel internal parallel model, Res. J. Environ. Toxicol. 9 (2015) 1–16.

[48] A.M. Georgescu, F. Nardou, V. Zichil, I.D. Nistor, Adsorption of lead(II) ions from aqueous solutions onto Cr-Pillared clays, App. Clay Sci. 152 (2018) 44–50.

[49] H.Y. Erbil, Surface Chemistry of Solid and Liquids Interfaces, Blackwell Publishers, Oxford, Malden, MA, 2006.

[50] A. Florido, C. Valderrama, J.A. Arévalo, I. Casas, M. Martínez, N. Miralles, Application of two sites non-equilibrium sorption model for the removal of Cu(II) onto grape stalk wastes in a fixed-bed column, Chem. Eng. J. 156 (2010) 298–304.